

Microstructure of low temperature grown AlN thin films on Si(111)

G. W. Auner^{a)} and F. Jin

Electrical and Computer Engineering Department, Wayne State University, Detroit, Michigan 48202

V. M. Naik

Department of Natural Sciences, University of Michigan–Dearborn, Dearborn, Michigan 48128

R. Naik

Department of Physics and Astronomy, Wayne State University, Detroit, Michigan 48202

(Received 20 July 1998; accepted for publication 11 February 1999)

AlN thin films were grown on HF-etched Si(111) substrates at 400–600 °C by plasma source molecular beam epitaxy. Reflection high energy electron diffraction and transmission electron microscopy studies show that AlN films grown at 400 °C form an initial amorphous region at the interface, followed by *c*-axis oriented columnar grains with slightly different tilts and twists. AlN films grown at 600 °C showed a significantly reduced amorphous region near the interface promoting an epitaxial growth of AlN with AlN[0001]||Si[111] and AlN[01 $\bar{1}$ 0]||Si[11 $\bar{2}$] orientations. However, all the films show numerous defects such as stacking faults, dislocations, and grain boundaries. © 1999 American Institute of Physics. [S0021-8979(99)00611-8]

INTRODUCTION

Aluminum nitride (AlN) is an important material with many potential applications, because of its wide band gap (6.2 eV), high dielectric strength, high temperature stability, chemical inertness, high thermal conductivity, and high acoustic velocity.¹ One of the main focuses of AlN research has been on its thin film piezoelectric properties for surface acoustic wave devices.^{2,3} Further, AlN thin films have also been used as buffer layers for the growth of high quality GaN⁴ and AlGaIn films.⁵ AlN films have been grown on silicon substrates using different growth techniques such as chemical vapor deposition (CVD),^{6,7} reactive sputtering,^{3,8} plasma assisted molecular beam epitaxy,^{9–11} and pulsed laser deposition.¹² The choice of Si as the substrate for the growth of AlN films has the advantage of its easy integration into the existing device technology. For many device applications, the AlN films must be single crystalline with a smooth surface. During the growth, the substrate temperatures have to be maintained at >800 °C in order to obtain good epitaxial AlN films. However, for developing new devices hybridized with Si devices, it is important to grow AlN films on Si substrates at low temperatures to avoid thermal damage to Si devices. Therefore, an investigation of the microstructure of the low temperature grown AlN films on Si substrates is important.

A few investigators have grown AlN films at lower substrate temperatures employing various methods.^{6–12} For example, Zhang *et al.*⁷ have synthesized highly *c*-axis oriented polycrystalline AlN films on Si(111) substrates via microwave excited electron cyclotron resonance assisted CVD at substrate temperatures ranging from 300 to 400 °C from the AlBr₃–N₂–H₂Ar gas system. Meng, Heremans, and Cheng⁸ have studied the growth of AlN on Si(111) at substrate temperatures ranging from 500 to 800 °C by ultrahigh vacuum

(UHV) reactive direct current (dc)-magnetron sputtering under a mixture of Ar and N₂ gases. Their results of transmission electron microscopy (TEM), both plan-view and cross-sectional studies demonstrate that AlN can be grown epitaxially on Si(111), with AlN[0001]||Si[111], and AlN[11 $\bar{2}$ 0]||Si[2 $\bar{2}$ 0]. The AlN/Si epitaxy was explained by a 5:4 coincidence growth rather than a lattice matching condition. The lowest temperature required to achieve epitaxy was determined to be ~600 °C, although a considerable in-plane alignment existed in the polycrystalline films grown at 500 °C. At higher growth temperatures, perhaps the surface mobility of the adatoms or precursors is increased and epitaxy is promoted. On the other hand, for growth at low temperatures, limited mobility of the adatoms leads to a polycrystalline (mosaic) texture with preferential columnar orientations.⁹ To our knowledge there have been no cross-sectional TEM studies reported in literature on low temperature grown AlN films on Si(111) substrates to reveal the initial stages of growth. In the present article, we report on the cross-sectional TEM studies of highly *c*-axis oriented AlN thin films grown by plasma source molecular beam epitaxy (PSMBE) deposition^{13,14} on Si(111) substrates at 400 and 600 °C. While the reflection high energy electron diffraction (RHEED) method was used for *in situ* structural characterization during the growth process, x-ray diffraction (XRD)/rocking curve measurements were used for *ex situ* characterization to determine the orientation and texture of the films. The surface morphology of the films was examined by atomic force microscopy (AFM). Cross-sectional TEM studies have been performed to examine the AlN/Si interface and its effect on the subsequent microstructure of the AlN film. A correlation is made between the TEM and RHEED/XRD observations.

EXPERIMENT

The AlN films were prepared using a PSMBE deposition system. Details of the deposition system are described

^{a)}Electronic mail: gauner@ece.wayne.edu

elsewhere.^{13,14} Briefly, the PSMBE system has a new and innovative MBE deposition source—a hollow cathode source which uses radio frequency (rf) power (300 W for this system) to generate a nitrogen/argon plasma. This deposition technique uses a magnetically enhanced hollow cathode lined with the target material. An argon/nitrogen plasma is formed within the hollow cathode. The secondary electrons are confined to the source hollow cathode and do not interact with the substrate, which is approximately 25 cm away. Furthermore, due to the extreme anisotropy of the kinetically ejected atoms perpendicular to the source wall and the hollow cathode tapered geometry, virtually no high-energy atoms or ions are directed to the substrate. Instead the atoms go through multiple collisions and thermalize. Ions are extracted from the source via an impeller or acceleration bias allowing a controlled energy deposition. Mass spectrometry energy analysis of the nonaccelerated ions ejected from the source indicates a Gaussian energy distribution about the approximate 1 eV range. The PSMBE source, in contrast to planar sputtering, allows enough adatom energy to create AlN (or other nitrides) crystals while minimizing damage to the underlying crystal. The base vacuum of the deposition system is approximately 5×10^{-10} Torr, the argon and nitrogen flow rates are respectively, 40 and 20 sccm. The dynamic pressure during growth is 1 mTorr. The dissociated nitrogen ions and the sputtered aluminum ions are accelerated by a dc biasing (-12 V for this system) toward the heated substrate, where they form AlN crystalline films.

The *n*-type Si(111) substrates were cleaned before loading into the chamber by standard Radio Corporation of America method and dipped in 10% HF for 30 s to remove the oxides on the surface. Previous studies^{15,16} have shown that this process passivates the Si(111) surface against oxidation by hydrogen termination of the Si bonds. The surface is known to be inert for several minutes in air and for several hours in UHV at room temperature. The surface passivation is lost if the substrate is heated to above 550 °C or by electron bombardment due to hydrogen desorption.¹⁷ Our previous studies on H-terminated Si(111) surface showed RHEED patterns with sharp and intense diffraction streaks along with the Kikuchi lines characteristic of a well ordered 1×1 Si(111) surface.¹⁸ We have also observed that the Si(111) surface remain unreconstructed even after heating up to 850 °C.

AlN films of 3000 Å thickness were grown at 400 and 600 °C. The deposition rate was approximately 0.5 Å/s based on a quartz crystal thickness monitor calibrated using a diamond stylus profilometer. The measured thickness of the film has an error of $\pm 10\%$. RHEED patterns were continuously monitored during the deposition to gauge the quality and surface structure of the film. Standard XRD ($\theta-2\theta$) scans and the rocking curve measurements were performed with a Rigaku powder diffractometer using Cu $K\alpha$ radiation. A Digital Instruments Nanoscope III Multimode AFM operating in the contact mode was used for AFM studies. TEM cross-section samples were prepared by bonding two films face to face, mechanical thinning, and ion milling. Atomic resolution TEM was performed on a JEOL 4000EX trans-

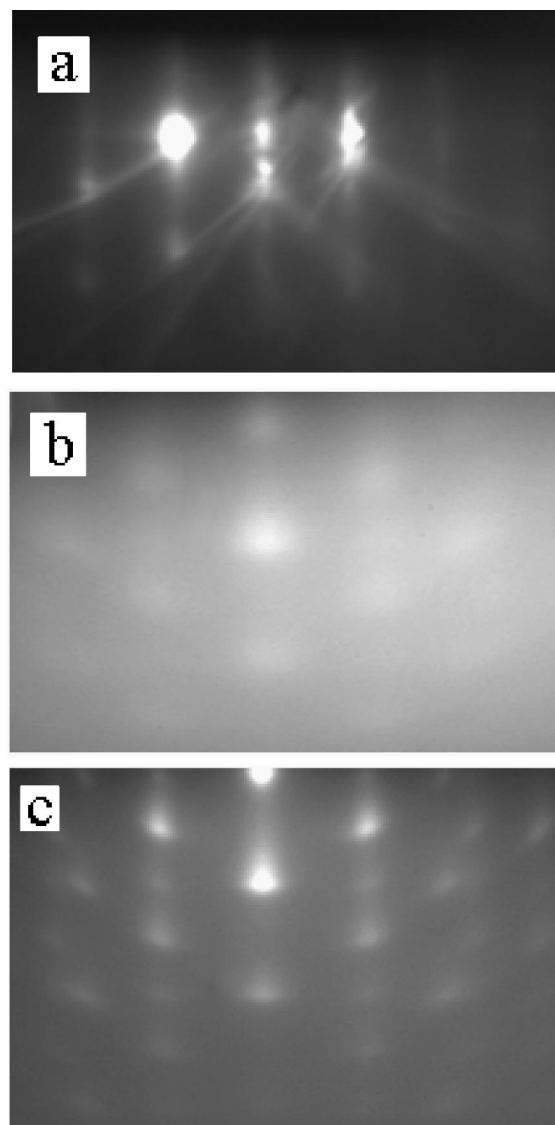


FIG. 1. RHEED patterns viewed along Si $\langle 112 \rangle$ azimuth, during AlN deposition at 400 °C: (a) Si, (b) after depositing 200 Å AlN, and (c) after depositing 3000 Å of AlN.

mission electron microscope, operating at 400 kV enabling a point-to-point resolution better than 1.8 Å.

RESULTS AND DISCUSSION

Figure 1(a) shows the RHEED pattern of a hydrogen terminated Si(111) surface observed along $\langle 110 \rangle$ azimuth of Si at room temperature. The presence of sharp and intense diffraction streaks along with Kikuchi lines indicates a well ordered Si(111) surface. AlN was deposited after the substrate was heated to 400 °C. During the initial deposition of AlN film, sharp streaks of Si(111) were replaced by a bright background, suggesting an amorphous growth. However, after a deposition of ~ 100 -Å-thick AlN film, faint diffraction spots appeared. For example, Fig. 1(b) shows the RHEED pattern after a deposition of 200-Å-thick AlN film. The pattern became sharper and intense with increasing film thickness. Figure 1(c) shows a snap shot of the RHEED pattern observed along Si $\langle 110 \rangle$ azimuth, when the film thickness was

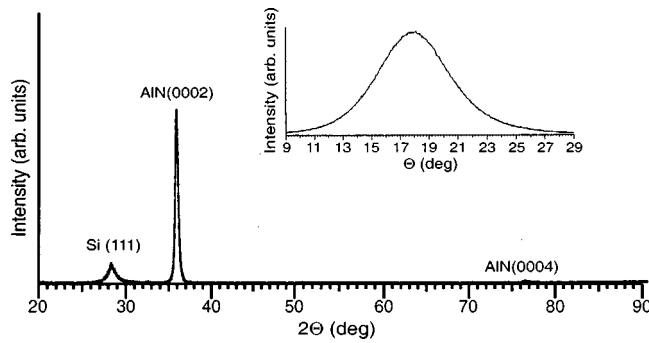


FIG. 2. θ - 2θ XRD scan of a 3000-Å-thick AlN film grown at 400 °C. Inset shows the rocking curve of AlN(0002) peak.

3000 Å. The RHEED pattern was also examined along the Si(112) azimuth. Surprisingly, the pattern was identical to the one observed along the Si(110) azimuth. Indeed, the pattern remained essentially the same when viewed along any azimuth of Si. The observed pattern can be indexed (explained later) as a superposition of both AlN[2 $\bar{1}\bar{1}0$] and AlN[01 $\bar{1}0$] zone axes patterns with c axis of AlN oriented along the film normal. The observation of a spotty pattern, which looks the same along any azimuth instead of diffraction rings, indicates that the film is not completely polycrystalline, but rather has a distribution of rotated columnar grains with c axis along the growth direction. In each grain, there is considerable in-plane, alignment similar to the results observed on AlN films grown at 500 °C by Meng, Heremans, and Cheng.⁸ Their plan-view TEM studies showed a readily perceptible remnant single-crystal selected area diffraction pattern (SADP). The dark-field micrographs taken with remnant AlN(10 $\bar{1}0$) spot showed randomly distributed crystals with a typical grain size of ~ 100 Å. Similar observations were made by Lei *et al.*¹⁹ in the case of highly oriented GaN polycrystalline films grown on Si(001) by electron cyclotron resonance microwave plasma-assisted MBE.

Figure 2 shows a θ - 2θ XRD scan of a 3000-Å-thick AlN film grown at 400 °C. The XRD pattern shows only AlN(0002) and (0004) peaks. The absence of other AlN reflections indicates a complete texture of the film with AlN[0001]||Si[111] in agreement with the RHEED observations. The full width at half maximum (FWHM) of AlN(0002) peak is $\sim 0.4^\circ$, as compared to 0.15° observed for Si(111) reflection. The broadening of AlN(0002) peak could be due to the presence of micro-stresses and/or to the small crystallite size. The rocking curve was also measured for further investigation of the degree of the c -axis orientation. The inset shows the rocking curve scan corresponding to AlN(0002) peak with a FWHM $\sim 5.7^\circ$. This rather large value of FWHM shows a considerable spread in the c -axis orientation of AlN columnar grains with respect to the film normal. AFM scans were done in order to see the effect of these grain structures on the film morphology. AFM scans on two different AlN films with thickness of 200 and 3000 Å grown on Si(111) at 400 °C are shown in Figs. 3(a) and 3(b), respectively. The 200-Å-thick AlN film shows a relatively smooth morphology with a root mean square (rms) roughness ~ 8 Å over an average lateral size of ~ 300 Å. In com-

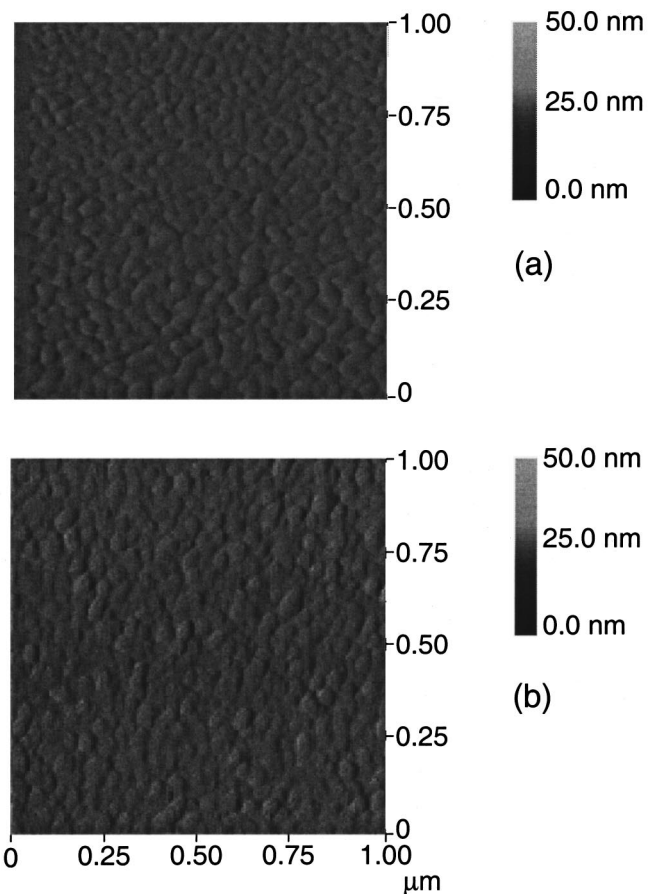


FIG. 3. AFM scans on two different AlN films with thickness of 200 and 3000 Å grown on Si(111) at 400 °C.

parison, the 3000-Å-thick film has a rms roughness ~ 15 Å over an average lateral size of ~ 400 Å. The grain size and roughness seems to increase with the increase in film thickness.

In order to confirm the inferences from RHEED and XRD observations, cross-sectional TEM studies were carried out on the above 3000-Å-thick AlN film grown on Si(111). These studies reveal how the initial stages of the growth controls the subsequent microstructure of the film. A cross-sectional image of the sample near the AlN/Si interface re-

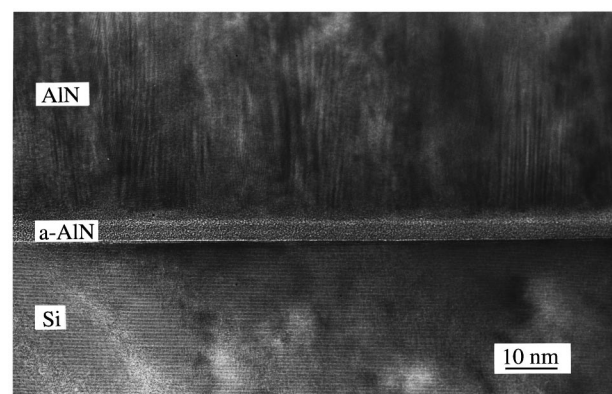


FIG. 4. A cross-sectional image near the AlN/Si interface region of the AlN film grown at 400 °C. The electron beam is parallel to Si[11 $\bar{2}$].

gion, with electron beam parallel to Si[112], is shown in Fig. 4. The image clearly shows an amorphous region of ~ 50 Å thickness, followed by growth of crystalline AlN. Kester *et al.*²⁰ have observed a similar initial amorphous region for a BN film grown on Si(100) substrate at 400 °C using electron beam evaporation with simultaneous bombardment of nitrogen and Ar ions. A similar observation has also been made by Yong *et al.*²¹ during the growth of AlN:H films on Si(100) substrates at room temperature by rf reactive sputtering. They suggest that the uniformly formed amorphous layer reduces the lattice mismatch and the short range ordering in the amorphous layer provides nucleation sites for the growth of *c*-axis oriented crystallites normal to the substrate. We believe that at lower substrate temperatures, the adatoms do not have enough mobility to align with the Si lattice for epitaxial growth, and hence, form an amorphous layer of AlN, perhaps mixed with Si in our films. However, we do not expect SiN formation at these lower temperatures and low ion energies. In fact, the amorphous layer is decreased as the substrate temperature increases indicating a condensed amorphous AlN region rather than a modification of the Si substrate (higher temperature data described later). Subsequently, crystalline AlN(0002) planes are seen to grow roughly parallel to the substrate surface very similar to the sputtered AlN films grown on glass substrates.²² It is believed that the preferential columnar orientation is due to the minimum surface energy of AlN(0002) relative to other faces.⁹

TEM results are in agreement with our RHEED observations, where only a bright background was seen during the initial stages of AlN growth indicating an amorphous film, followed by diffraction spots corresponding to a crystalline AlN. A careful and closer look at the amorphous region under high resolution TEM revealed that the thickness of the amorphous AlN region is not uniform but varied by $\pm 10\%$ over a lateral regions of ~ 200 Å. These local variations in thickness seem to create a waviness in the AlN(0002) planes grown subsequently which leads to a significant tilting and twisting of the *c*-axis oriented grains relative to the film normal. In fact, the vertical fringes observed in the TEM micrograph (Fig. 4) are the rotational Moiré patterns²³ due to the overlapping lattice planes of slightly tilted and twisted grains with respect to the film normal. From the fringe width we estimate that the angle of rotation between the grains to be $\sim 14^\circ$ with a grain size of ~ 200 Å. A high resolution TEM micrograph of only AlN region, with electron beam parallel to Si[112], is shown in Fig. 5. The micrograph reveals numerous defects such as stacking faults, dislocations, and grain boundaries, which are formed when grains containing (0002) AlN planes with slightly different tilts and twists join together.

A SADP taken around the interfacial region of AlN/Si is shown in Fig. 6 along with its indexed pattern. The diffraction pattern shows overlapping Si[112] and predominantly AlN[2 $\bar{1}\bar{1}0$] and AlN[01 $\bar{1}0$] zone axis patterns. This indexing of AlN also applies to the RHEED pattern described earlier. In addition, the pattern also reveals the presence of other misaligned regions. Diffraction spots observed along the AlN(0001) direction are significantly intense with their

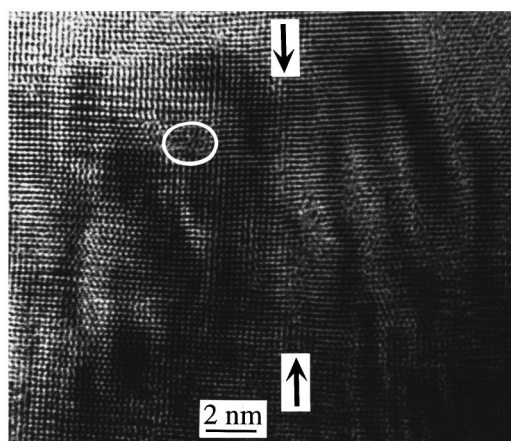


FIG. 5. A high resolution TEM image of only AlN, with electron beam parallel to Si[112]. The film shows numerous defects, for example, the arrow marks indicate a boundary a region between adjacent the AlN grains with slightly different shift/tilt in the (0002) AlN planes. The circle shows a region of stacking fault.

intensity distributed along an arc of a circle. This implies that the growth is highly *c*-axis oriented with a considerable spread in the *c*-axis orientation with respect to the film normal. This indeed accounts for the observed large FWHM for AlN(0002) XRD rocking curves.

The interpretation that the observed AlN amorphous region is due to low mobility of the adatoms was further tested by performing TEM cross-sectional studies on a 1000-Å-thick AlN film grown on hydrogen terminated Si(111) substrate heated to 600 °C. All other growth conditions were identical to those of AlN films grown at 400 °C. A high-resolution cross-sectional TEM image viewed with electron beam parallel to Si[1 $\bar{1}0$] is shown in Fig. 7. The amorphous region in this film is significantly reduced compared to the AlN film grown at 400 °C, allowing an epitaxial growth on Si(111) surface. Indeed the SADP (inset) shows only AlN[2 $\bar{1}\bar{1}0$] spots along with the overlapping Si[1 $\bar{1}0$] zone axis patterns. The epitaxial relationships are AlN[0001]||Si[111], and AlN[01 $\bar{1}0$]||Si[112] similar to the results of Refs. 8 and 12. The increased temperature seems to promote epitaxial growth. However, a significant waviness and tilting of the AlN(0002) planes can be still observed in the micrograph, along with the presence of numerous stacking faults, dislocations, and grain boundaries. XRD θ - 2θ scan of this film shows only AlN(0002) and AlN(0004) peaks very similar to that of Fig. 2, but with a decreased FWHM $\sim 4.4^\circ$ compared to 5.7° for AlN film grown at 400 °C for AlN(0002) rocking curve. The film morphology, as determined by AFM, is also very similar to those grown at 400 °C with a rms roughness of ~ 10 Å over a lateral size of 400 Å.

In summary, we have studied AlN thin films grown on HF-etched Si(111) substrates by PSMBE deposition at substrate temperatures of 400–600 °C. RHEED and TEM studies show that at 400 °C, AlN film forms an initial amorphous region (~ 50 Å) at the interface, followed by *c*-axis oriented columnar grains (~ 200 Å) with slightly different tilts and twists. The grain size seems to increase with increase of film

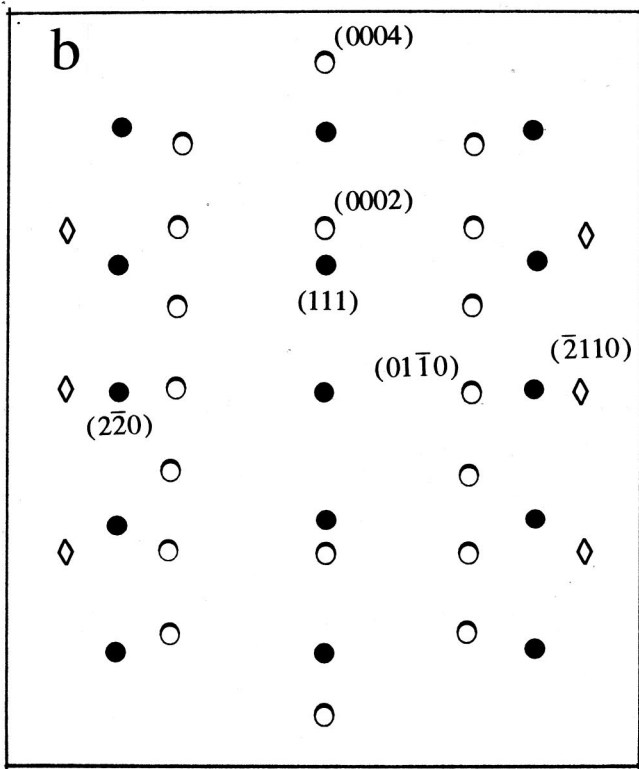
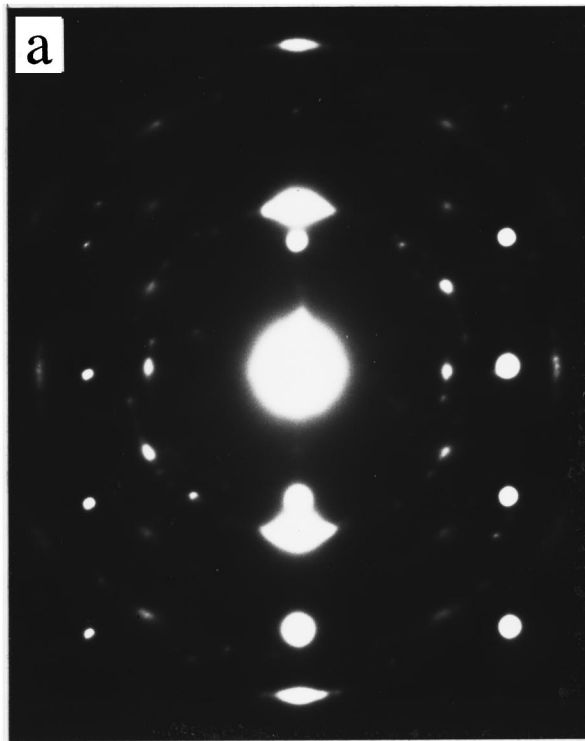


FIG. 6. (a) SADP of overlapping Si and AlN regions, and (b) indexed pattern of (a). ●, ○, ◇ are spots corresponding to Si[112̄], AlN[21̄1̄0], and AlN[01̄1̄0] zone axis patterns. Remaining spots in (a) are due to mis-oriented grains and double diffraction.

thickness. AlN film grown at 600 °C showed a significantly reduced amorphous region near the AlN/Si interface promoting an epitaxial growth of AlN[0001]||Si[111] with AlN[01̄1̄0]||Si[112̄]. However, all the films show numerous

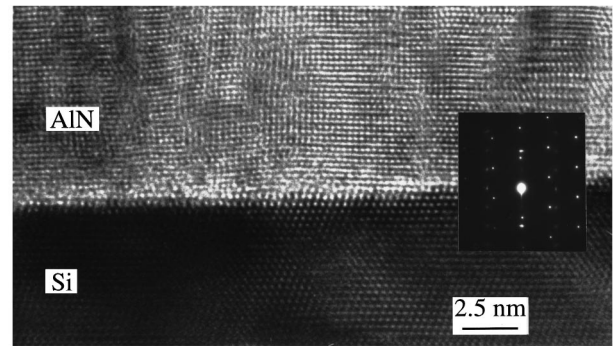


FIG. 7. A high resolution TEM image near the AlN/Si interface region of the AlN film grown at 600 °C, with electron beam parallel to Si[01̄1̄].

defects such as stacking faults, dislocations, and grain boundaries.

ACKNOWLEDGMENTS

This work was supported by National Science Foundation Grant No. EEC-9420568. The TEM studies were done at the University of Michigan Electron Microbeam Analysis Laboratory.

¹S. Strite and H. Morkoc, *J. Vac. Sci. Technol. B* **10**, 1237 (1992).
²H. Okano, N. Tanaka, K. Shibata, and S. Nakano, *Jpn. J. Appl. Phys., Part 1* **32**, 4052 (1993).
³H. Okano, Y. Takahashi, T. Tanaka, K. Shibata, and S. Nakano, *Jpn. J. Appl. Phys., Part 1* **31**, 3446 (1992).
⁴H. Amano, N. Sawaki, I. Akasaki, and Y. Toyoda *Appl. Phys. Lett.* **48**, 353 (1986).
⁵F. A. Ponce, J. S. Major, Jr., W. E. Plano, and D. F. Welch, *Appl. Phys. Lett.* **65**, 2302 (1994).
⁶H. Khan *et al.*, *J. Mater. Sci.* **39**, 4314 (1994).
⁷W. Zhang, Y. Someno, M. Sasaki, and T. Hirai, *Jpn. J. Appl. Phys., Part 2* **32**, L116 (1993).
⁸W. J. Meng, J. Heremans, and Y. T. Cheng, *Appl. Phys. Lett.* **59**, 2097 (1991); *Mater. Res. Soc. Symp. Proc.* **242**, 469 (1992).
⁹K. S. Stevens, A. Ohtani, M. Kinniburgh, and R. Beresford, *Appl. Phys. Lett.* **65**, 321 (1994).
¹⁰M. Miyauchi, Y. Ishikawa, and N. Shibata, *Jpn. J. Appl. Phys., Part 2* **31**, L1714 (1992).
¹¹A. Bourret, A. Barski, J. L. Rouviere, G. Renaud, and A. Barbier, *J. Appl. Phys.* **83**, 2003 (1998).
¹²R. D. Vispute, J. Narayan, H. Wu, and K. Jagannadham, *J. Appl. Phys.* **77**, 4724 (1995).
¹³G. W. Auner, T. D. Lenane, F. Ahmad, R. Naik, P. K. Kuo, and Z. Wu, in *Wide Band Gap Electronic Materials* (Academic, Netherlands, 1995), p. 329.
¹⁴P. K. Kuo, G. W. Auner, and Z. L. Wu, *Thin Solid Films* **253**, 223 (1994).
¹⁵P. Dumas, Y. J. Chabal, and G. S. Higashi, *Phys. Rev. Lett.* **65**, 1124 (1990).
¹⁶S. S. Iyer, M. Arienzo, and E. de Fresart, *Appl. Phys. Lett.* **57**, 893 (1990).
¹⁷T. Takahagi, A. Ishitani, H. Kuroda, Y. Nagasawa, H. Ito, and S. Wakao, *J. Appl. Phys.* **68**, 2187 (1990).
¹⁸R. Naik, C. Kota, B. U. M. Rao, and G. W. Auner, *J. Vac. Sci. Technol. A* **12**, 1832 (1994).
¹⁹T. Lei, M. Fanciulli, R. J. Molnar, T. D. Moustakas, R. J. Graham, and J. Scanlon, *Appl. Phys. Lett.* **59**, 944 (1991).
²⁰D. J. Kester, K. S. Ailey, R. F. Davis, and K. L. More, *J. Mater. Res.* **8**, 1213 (1993).
²¹Y. J. Yong, J. Y. Lee, H. S. Kim, and J. Y. Lee, *Appl. Phys. Lett.* **71**, 1489 (1997).
²²M. A. Odintzov, N. I. Sushentzov, and T. L. Kudryavtzev, *Sens. Actuators A* **28**, 203 (1991).
²³H. Hirsch, A. Howie, R. B. Nicholson, D. W. Pashley, and M. J. Whelan, *Electron Microscopy of Thin Crystals* (Krieger, Malabar, FL, 1977).